Sixth International Conference on Durability of Concrete Structures **Paper Number ICC24**
18 - 20 July 2018
University of Leeds, Leeds, West Yorkshire, LS2 9JT, United Kingdom

Impact of Portlandite on Alkali-Silica Reaction of Pyrex Glass and Blastfurnace Slag Aggregate

N. Noguchi, T. Kajio, Y. Morinaga, Y. Elakneswaran and T. Nawa
Graduate School of Engineering, Hokkaido University, Sapporo-shi, Hokkaido, Japan

T. Ayan
Graduate School of Environmental and Life Science, Okayama University, Okayama, Japan

ABSTRACT

In this study, it is investigated the effect of Ca ion on dissolution and reaction products in alkaline environment using Pyrex glass showing ASR expansion and blast furnace slag fine aggregate suppressing ASR. It is reported that Ca plays a role in the dissolution and polymerization of silica, and is therefore an important factor in ASR. For each sample, calculation of dissolution rate and analysis of solid phase product by ^{29}Si MAS NMR and XRD/Rietveld analysis, and liquid phase analysis by ICP-AES were performed. As a result, it was confirmed that addition of Ca has an influence on dissolution behavior of PG and BFS. In the reaction of PG, addition of Ca promotes the polymerization reaction of silica and increases the amount of N-S-H which has expandable and contributes to deterioration mechanism. On the other hand, in BFS, the dissolved silica did not polymerize and N-S-H did not form. It was suggested that the difference in ASR reactivity between PG and BFS is due to the difference in the reaction behavior.

Keywords: ASR, Portlandite, Reactive glass, Blast Furnace Slag, ^{29}Si MAS NMR, XRD/Rietveld analysis

1.0 INTRODUCTION

Alkali silica reaction (ASR) is one of the serious problems of deterioration of concrete structures, and is known as a problem of lowering the durability of concrete. When reactive silica included aggregates react with the high pH pore solution of concrete, the silica dissolves into the pore solution containing K, Na, Ca ions to form the ASR products such as alkali calcium silicate (Ca-N/K-S-H) and alkali silicate (N/K-S-H). The ASR product increases in volume with water absorption and generates an expansive pressure inside the aggregate, causing cracking and loss of strength of concrete.

A lot of research about ASR have been conducted so far, but the reaction mechanism of ASR is not clear yet. Ichikawa (Ichikawa and Miura, 2007) proposes a mechanism in which a reactive rim is formed around the aggregate and cracks is generated by the swelling pressure from the inside. However, there are reports that ASR occurs without reaction rim. Therefore, it is necessary to discuss the reaction mechanism of ASR in detail and establish it. In recent studies, on the reaction products of ASR, it is reported that N/K-S-H is formed after the formation of C-S-H and C-N/K-S-H, and N/K-S-H affect expansion (Hou, Struble and Kirkpatrick, 2004). Since ASR products are formed from concrete aggregate, it is important to discuss the reactivity of aggregates and reaction products.

On the other hand, Ca is known as important factor of ASR. Rajabipour (Rajabipour *et al*., 2015) reported Ca contained in concrete plays a role of promoting the process of dissolution of silica which is rate determining step of ASR and a catalyst of polymerization of silica. Leemann (Leemann *et al*., 2011) reported that the structure of the ASR product was influenced by the amount of CH added, using micro silica as a model aggregate. The authors have studied dissolution of silica, ASR products in samples using Pyrex glass (Noguchi *et al*., 2018).

Recently, using of blast furnace slag (BFS) as concrete aggregate is expected. Blast furnace slag fine aggregate is one in which blast furnace slag is crushed and sized and an anti-bonding agent is added. Advantages of BFS include reduction of environmental load, suppression of ASR and drying shrinkage of concrete. There are several studies on alkali-activated slag as a binder of concrete (Wang and Scrivener, 1995) (Richardson *et al*., 1994), but there are few articles discussing the reactivity of BFS, and the mechanism of ASR suppression effect by using BFS is not clear. Since concrete aggregate can be a base material for ASR product, it needs to be thoroughly studied. In addition, study on the reaction with Ca which affects the dissolution polymerization process of silica has not been advanced yet.

It is expected that new findings can be gained in the mechanism of ASR or the mechanism by which BFS is used by comparing the reactivity of the model

aggregate showing expansion behavior and BFS suppressing expansion and reaction products and Ca.

In this study, focusing the chemical reaction and products of ASR, Pyrex glass (PG) which shows swelling behavior and has been used a lot as research subject as a model aggregate (Heisig *et al*., 2016) (Baingam, 2016), and two types of BFS were used. Since the main components in the sample are identical to the components of ASR in mortar or concrete, similar chemical reaction can be expected. The reactivity of each aggregates and reaction products were discussed. Moreover, the amount of CH added was changed to discuss the influence of Ca. Several measurements were conducted for each sample, ICP-AES, ^{29}Si MAS NMR, XRD/Rietveld analysis.

2.0 MATELIALS AND METHODS

2.1 Materials and sample preparation

Pyrex glass (PG) 7740 of Iwaki Glass and two kinds of BFS (A and B) produced at the steel mills in Japan were used. Table 1 showed the chemical composition of PG and BFS. From the XRD/Rietveld analysis of unreacted BFS, B is composed of amorphous, while A contains 12% Melilite. Melilite is a solid solution of Gehlenite ($Ca_2Al_2SiO_7$) and Akermanite ($Ca_2MgSi_2O_7$). PG and BFS were ground and sieved to a range of particle sizes from 300 to 150 μm. The special grade reagents of portlandite (CH) and NaOH from Kanto Chemical were used.

Table 1. Chemical composition of PG and BFS (%)

PG		BFS		
			A	B
SiO_2	80.9	CaO	37.85	37.47
B_2O_5	12.6	SiO_2	26.97	29.81
Al_2O_3	2.3	Al_2O_3	11.04	9.95
Na_2O+K_2O	4.0	Na_2O	9.62	10.59
		MgO	6.12	3.68
		P_2O_5	5.62	6.05
		SO_3	1.3	0.49
		K_2O, MnO, TiO_2, Fe_2O_3	>1.0	>1.0

The amount of CH added with 5g of PG is 1.54, 0.77, 0.385g, and 5g of BFS is 1.54, 0.513g. Solid sample were mixed in 20 ml of 1 M NaOH solution. The reacted samples were decanted into several 30 ml polyethylene tubes and placed in an oven at 70 °C to speed up the reaction. After that, samples were filtered through a 45μm filter to separate solid and liquid sample. The solid sample was immersed in acetone for an hour to stop the reaction. Free water in the sample was extracted by immersing the sample in acetone. After that, samples were dried in an oven at 40 ºC for 3 hours.

In order to calculate the dissolution rate of BFS, the sample was fired in accordance with the previous report (Ishikawa *et al*., 2015). Upon calcination, a program was used in which the temperature was raised to 900 ° C. in 30 minutes and then maintained for 30 minutes.

2.2 Experimental procedure

The obtained sample was measured under the following conditions. For the detail measurement of the PG sample, refer to our previous work (Noguchi *et al*., 2018).

The separated solids were ground to fine powders (particle sizes smaller than 150 μm) and conducted X-ray diffraction (XRD). The samples were analysed with Rigaku X-ray generator using CuKα radiation at a scanning rate of 1°2θ per min and a step size of 0.02 °2θ the ranging from 5 to 70 °2θ. Corundum was used as a standard substance. Siroquant Version 4.0 manufactured by Sietronics was used for Rietveld analysis.

Before the XRD measurement, add 10wt% of corundum(Al_2O_3) to a part of the PG samples and mix for 10 minutes to make it homogeneous. Samples with corundum added were used only for XRD. In Rietveld analysis for PG samples, targets were portlandite, and corundum. The results of Rietveld analysis were corrected by ignition loss.

On the other hand, for BFS samples, Corundum is not added, and the mineral amount was calculated by the external standard method using Eq. (1) and Eq. (2). Melilite, Merwinite, Portlandite, Lime (only for crystallized samples) were used as targets.

$$G = \frac{s\rho V^2 \mu}{c} \quad (1)$$

$$c_j = \frac{s_j \rho_j V_j^2 \mu_{sample}}{G} \quad (2)$$

where: G is factor of standard substance (cm^5/wt%); s is scale factor; ρis density (g/cm^3); V is unit cell volume (cm^3); μ is mass absorption coefficient (cm^2/g); c is 100 (wt%); c_j is crystal amount of compound j (%)

As described above, in BFS sample, it is necessary to fire a part of the sample in order to calculate the dissolution rate. Therefore, in this paper, external standard method which does not add Corundum to sample and can also use for other measurements was used. It has been reported that the analysis by the internal standard method and the external

standard method in the cement system generally agree (Sagawa *et al*., 2015).

The ^{29}Si MAS NMR experiment was conducted by a MSL 400 9.4 T BRUKER operating with frequency of 79.486 MHz for ^{29}Si at room temperature to investigate the structure of the solids. The Q_8M_8 ($Si(CH_3)_8Si_8O_2$) produced by Wako Pure Chemical Industries was used as a reference material for the ^{29}Si-NMR chemical shifts at 12.4 ppm. The analysis conditions were as follows: a 30° pulse length of 1.7μs and 4kHz of the number of rotation. ^{29}Si recycling delay of 15 s and 1680 scans for PG sample, 3s and 3660 scans for unreacted BFS, 5s and 2160 scans for BFS sample. Win-nuts program was used for the analysis of ^{29}Si MAS NMR data.

For ICP-AES analysis, ICPE9000 manufactured by Shimadzu Corporation was used. The liquid samples were diluted by 1000 or 10000 times for PG sample, 200 or 2000 times for BFS sample and the concentration of Si and Ca were measured. Silicon standard solution and metals standard solution manufactured by Kanto Chemical were used for reference material.

3.0 RESULTS AND DISCUSSIONS

3.1 Chemical reaction and products of Pyrex glass and portlandite

The dissolution rate of PG and the amount of remaining CH as function of reaction time are shown in Fig. 1. The amount of remaining CH was calculated by the results of XRD/Rietveld analysis and corrected using the result of the loss on ignition. The dissolution rate was calculated from the measurement results of ^{29}Si MAS NMR and ICP-AES. As shown in figure, the amount of CH decreased very rapidly in 24 hours and then almost disappeared after 120 hours. The dissolution rate of PG does not depend on the amount of CH added for the reaction until 72 hours, the difference in dissolution rate due to the amount of CH addition is small. However, the dissolution rate increases with the amount of CH addition until 120 hours and then become constant. The initial amount of CH strongly affects the dissolution rate of PG, but the behavior or trend of dissolution is independent of CH content. The formation of reaction products is investigated using ^{29}Si MAS NMR measurement. Regarding the ASR products, it is reported that calcium silicate hydrate (C-S-H), calcium alkalis silicate hydrate (C-Na/K-S-H), alkalis silicate hydrate (Na/K-S-H) are the main ASR products (Rajabipour *et al*., 2015), (Hou, Struble and Kirkpatrick, 2004), (Kim and Olek, 2014). Since these products are primarily present as amorphous products, ^{29}Si MAS NMR measurement is used to describe their structure and quantitative measurements (Leemann *et al*., 2011), (Cong, Kirkpatrick and Diamond, 1993).

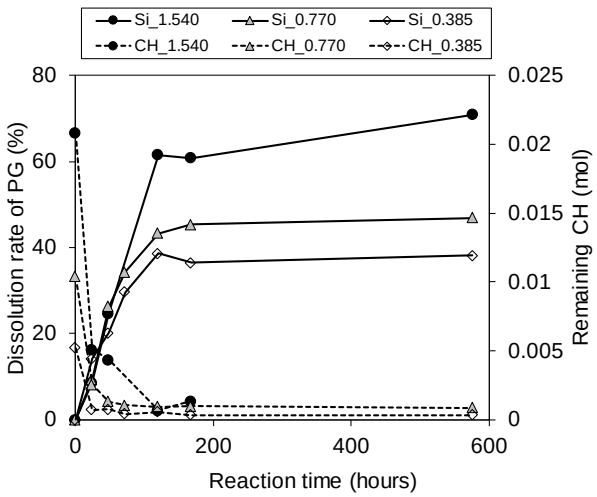

Fig. 1. The dissolution rate of PG and the reaction of CH for PG+NaOH+CH with 0.385, 0.77 and 1.54 g of CH contents

The ^{29}Si has different chemical shift depending on the number of silica polymerized via oxygen. The ^{29}Si chemical shifts of the signals were analyzed using the Q^n classification. Here, the silica tetrahedron is connected to n number of silicas tetrahedra where n varying from 0 to 4. Some studies have reported the presence of Q^1 and Q^2 in the alkali incorporated C-S-H (C-N/K-S-H) and C-S-H (Kim and Olek, 2014). Moreover, Hou (Hou *et al*., 2004) and Kirkpatrick (Kirkpatrick *et al*., 2005) suggested that the kanemite ($NaHSi_2O_5 \cdot 3H_2O$), a crystal form of alkalis silicate hydrate (N-S-H), represents as an ASR product which have Q^3 sites. In addition, Garcia (Garcia-Diaz *et al*., 2006) reported that the formation of Q^3 and the pore volume are correlated with aggregate expansion. Therefore, in this study, from ^{29}Si MAS NMR measurements, the sum of Q^1 and Q^2 obtained is attributed to C-S-H and C-N-S-H while Q^3 is referred to N-S-H.

Figure 2 shows the ^{29}Si MAS NMR spectrum of PG sample with CH and without CH for 168 hours along with the spectrum of unreacted PG. Each signal of the spectrum was classified as Q^n based on report by Baingam (Baingam *et al*., 2015). The unreacted PG shows a broad signal at -110 ppm correspond to Q^4 which refers the presence of amorphous SiO_2. The signals of PG sample without CH for 168 hours are so similar to that of unreacted PG, indicates the negligible amount of reaction products in the absence of CH and the silica dissolved from PG exist in liquid phase. This agrees with results reported by Leemenn (Leemann *et al*., 2011) and Baingam (Baingam *et al*., 2015). On the other hand, the sharp signal of Q^2 at -84 ppm and a broad signal of Q^3 at -95 ppm were observed for the reaction of each sample of PG with CH for 168 hours. Generation of C-S-H has also been confirmed from the XRD pattern. Since Q^3 and Q^4 are broad signals, they overlap in this figure. The signals of Q^2 and Q^3 are attributed to the alkali silica reaction

products. In the sample with a large addition amount of CH, the signal of Q^4 becomes lower.

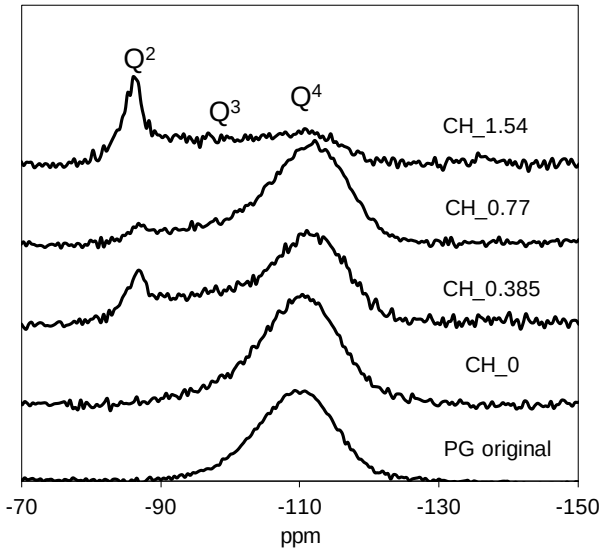

Fig. 2. ^{29}Si MAS NMR spectra of PG, and PG+NaOH and PG+NaOH+CH after 168 hours of reaction

More details description of PG dissolution and ASR products formation including thermodynamic modelling work were described our previous work (Noguchi *et al*., 2018).

3.2 Chemical reaction and products of blast furnace slag aggregate and portlandite

Dissolution of BFS in the presence of portlandite

Figure 3 shows the dissolution rate of BFS calculated from the XRD/Rietveld analysis of the sample crystallized. In samples with a large addition amount of CH, the time until the dissolution rate becomes constant is long. It was confirmed that BFS had reactivity with NaOH solution and CH. At the initial stage of the reaction up to 168 hours, the dissolution rate is lowered by adding CH. It was confirmed that behavior of dissolution rate is different between PG and BFS. In addition, the reaction rate under the same conditions is slightly higher for BFS containing more amorphous.

Figure 4 shows the liquid phase Ca and Si ion concentration of each sample calculated from the ICP-AES measurements. It is confirmed that the concentration of Ca and Si are low in each sample. Therefore, Si and Ca dissolved from BFS exists not in the liquid phase but in the solid phase. The tendency of Si concentration is different from that of PG. Also, the type of BFS and the amount of CH addition do not affect ion concentration.

Composition and structure of products formed from BFS

Figure 5 shows the ^{29}Si MAS NMR spectrum of BFS react with and without CH for 672 hours along with the spectrum of unreacted BFS.

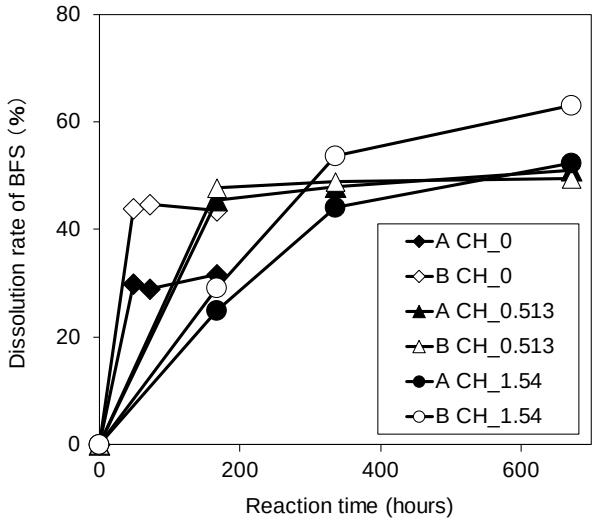

Fig. 3. The dissolution rate of BFS for BFS+NaOH+CH system with 0.513g and 1.54 g of CH contents

From Fig.5, unreacted BFS shows broad signal of Q^0 of -74 ppm in both A and B (Wang and Scrivener, 2003). The chemical bonding state of silica in the unreacted state is largely different between PG and BFS. In addition, unreacted and post-reaction signals are almost overlapped. Considering with Fig.1 and Fig. 2, since the bond state of Si in the unreacted state is Q^0, it is conceivable that dissolution behavior differs from that of conventional model aggregate having Q^4. At 28days, Q^1, Q^2 and Q^3 attributed to C-S-H or N-S-H were not formed in the BFS B sample. In the sample of BFS A, a slight signal of Q^1 is observed and the formation of C-S-H can be confirmed, but the production amount is very small. Furthermore, it is a major difference from PG that N-S-H contributing to expansion is not generated. It was confirmed that polymerization of silica did not occur despite the fact that Ca was sufficiently present. It is also shown that addition or addition of CH does not affect the polymerization of silica. Especially, it is considered that generation of N-S-H, which is supposed to contribute to expansion by ASR, is largely affecting the ASR suppression mechanism.

The XRD spectrum of each sample is shown in Fig. 6. First, peaks of C_4AH_{13} at 10.5° and katoite at 32.5° and C-S-H were observed in all sample. In the sample to which CH was added, the peak of CH was seen even on 28days and it showed a tendency different from that of PG. The external Ca source is necessary for the production of C_4AH_{13} and katoite. However, the peaks of C_4AH_{13} and katoite were all small, and it was confirmed that most of the products other than them were amorphous. In BFS B, since only Q^0 has been confirmed by ^{29}Si MAS NMR, the amount of C-S-H is considered to be very small, and it is necessary to investigate in the future.

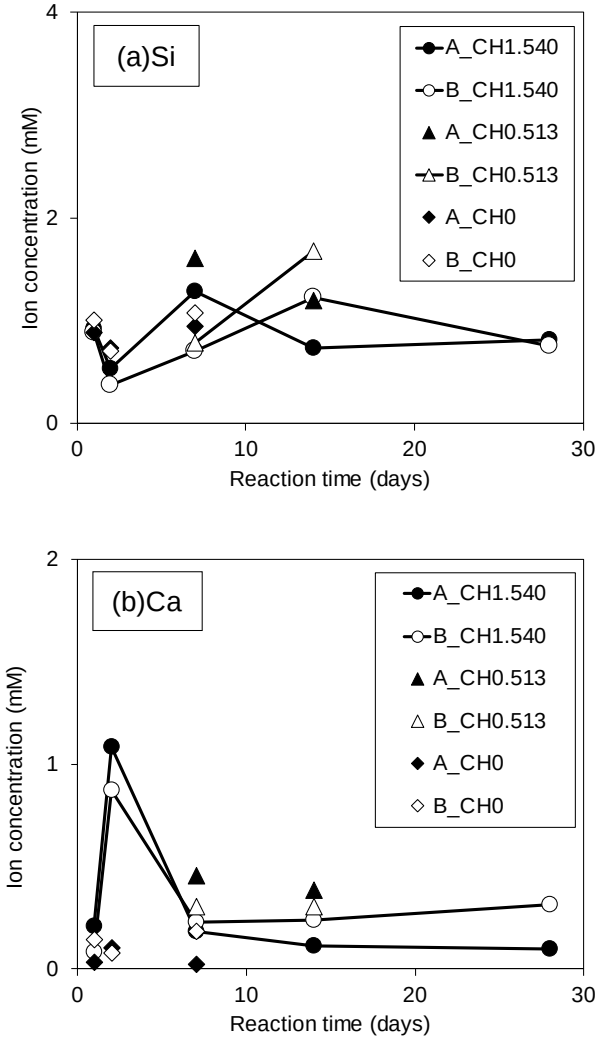

Fig. 4. Concentration of silica and calcium ions in liquid phase for BFS+NaOH+CH system with 0.513g and 1.54 g of CH contents. (a) silica (b) calcium

Regarding the reaction product, C(-N)-S-H and N-S-H are generated from PG, and the amount of production increases according to the amount of CH addition. On the other hands, N-S-H was not produced from BFS, and products could not be identified from XRD, NMR except for a few C-S-H C_4AH_{13} and katoite. Furthermore, the bonding state of Si in the unreacted sample is Q^0 in BFS and Q^4 in PG, and there is a difference in bonding state of silica before reaction. Rajabipour (Rajabipour *et al.*, 2015) summarized the dissolution and polymerization of silica having a bond of Q^4, but BFS does not have silica bonds, and it is conceivable that it is dissolved and polymerized by a mechanism different from that. Also, in the PG sample, the mechanism that N-S-H is generated after CH disappears is reported in our previous work. In BFS, it is possible to point out that N-S-H may not be generated because CH always remains.

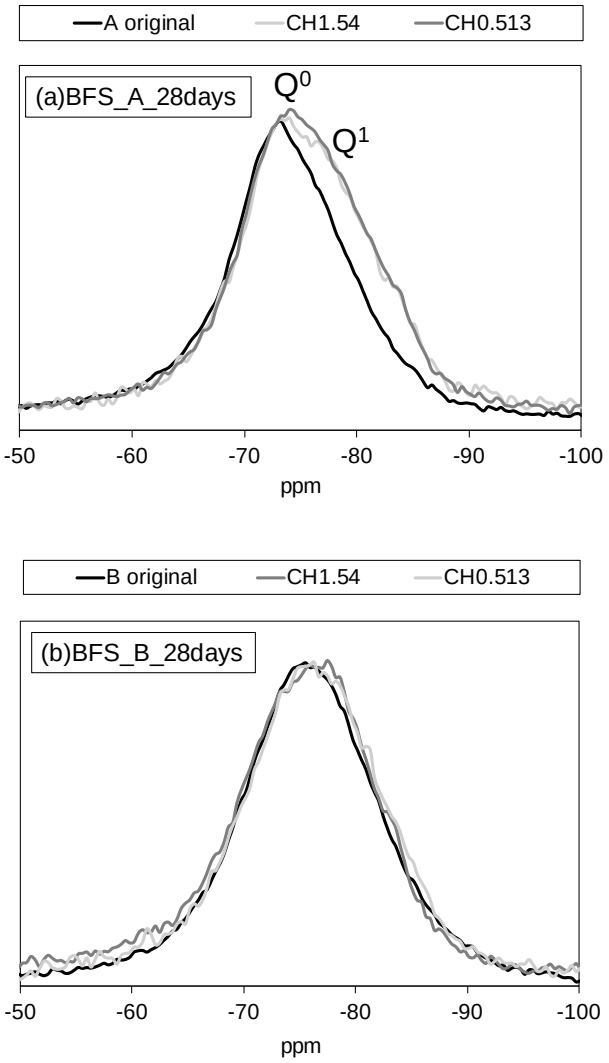

Fig. 5. Comparison of ^{29}Si MAS NMR spectra of BFS sample. (a) BFS_A (b) BFS_B

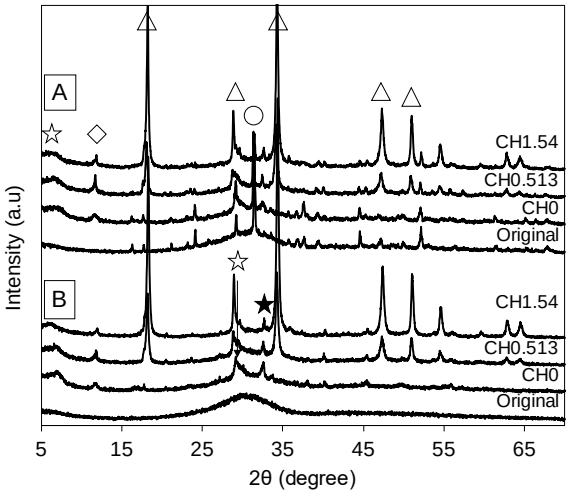

Fig. 6. XRD patterns for BFS+NaOH+CH system reacted for 28days (672hours) with 0.513g and 1.54 g of CH contents (◇ =C_4AH_{13} ○ =Melilite △ =Portlandite ★=Katoite)

In this way, it was confirmed that there was difference in product between PG and BFS. Also, the effects of CH on dissolution and product of aggregate are also different. It is suggested that generation of N-S-H which is considered to contribute to expansion by ASR, in particular, leads to ASR suppression effect of BFS. However, it is unknown whether amorphous produced from BFS contributes to expansion at all in the long term under actual circumstances is a future task.

4.0 CONCLUSIONS

In this study, we investigated the influence of Ca in ASR using PG as reactive glass and BFS. The presence and amount of CH have great effects on the dissolution of silica, while the behaviour of dissolution is different. In PG sample, the amount of C(-N)-S-H and N-S-H increase with the amount of CH. On the other hand, in BFS sample, only C-S-H is formed. It is suggested that the production of N-S-H affected the expansion of ASR. It was suggested that not generating N-S-H greatly affects ASR suppression effect by BFS.

References

Ichikawa. T, Miura. M, 2007. Modified model of alkali-silica reaction. Cement and Concrete Research. 37. 1297-1297.

Hou. X, Struble. L. J, Kirkpatrick. R. J, 2004. Formation of ASR gel and the roles of C-S-H and portlandite. Cement and Concrete Research. 34(9). 1383-1696.

Rajabipour. F, *et al*., 2015. Alkali-silica reaction: Current understanding of the reaction mechanisms and the knowledge gaps. Cement and Concrete Research. 76. 130-146.

Leemann. A, *et al*., 2011. Alkali-Silica reaction: The Influence of calcium on silica dissolution and the formation of reaction products. Journal of the American Ceramic Society. 94(4). 1243-1249.

Noguchi, *et al*. 2018. Influence of portlandite on Pyrex glass dissolution and the formation of alkali silica chemical reaction products. Journal of the American Ceramic Society. (doi/10.1111/jace.15719)

Ishikawa. R, *et al*., 2015. A study on validation of combined of crystallization by heat treatment and quantitative XRD-Reitveld method for determining hydration degree of blast-furnace-slag in slag-blended cement. Cement Science and Concrete Technology. 69. 76-81. (Japanese)

Sagawa. T, *et al*. 2015. Hydration analysis and phase composition of cement-based materials by x-ray diffraction/Rietveld method using an external standard. Cement Science and Concrete Technology. 68. 46-52. (Japanese)

Kim. T, Olek. J, 2014. Chemical sequence and kinetics of alkali-silica reaction part II. A thermodynamic model. Journal of the American Ceramic Society. 97(7). 2204-2212.

Cong. X, Kirkpatrick. R. J, Diamond. S, 1993. ^{29}Si MAS NMR Spectroscopic investigation of alkali silica reaction product gels. Cement and Concrete Research. 23(4). 811-823.

Garcia-Diaz. E, *et al*., 2006. Mechanism of damage for the alkali–silica reaction. Cement and Concrete Research. 36. 395-400.

Wang. S, Scrivener. K. L, 2003. ^{29}Si and ^{27}Al NMR study of alkali-activated slag. Cement and Concrete Research. 33. 769-774.